ISSN 1070-3284, Russian Journal of Coordination Chemistry, 2019, Vol. 45, No. 11, pp. 767–775. © Pleiades Publishing, Ltd., 2019.
Russian Text © The Author(s), 2019, published in Koordinatsionnaya Khimiya, 2019, Vol. 45, No. 11, pp. 663–671.

Intramolecular Nonvalent Interactions in the $Eu^{II}_2Eu^{III}(\mu\text{-}OR^F)_2(\mu_2\text{-}OR^F)_3(\mu_3\text{-}OR^F)_2(DME)_2$ Complex

R. V. Rumyantsev[a] and G. K. Fukin[a, *]

[a] *Razuvaev Institute of Organometallic Chemistry, Russian Academy of Sciences, Nizhny Novgorod, Russia*

**e-mail: gera@iomc.ras.ru*

Received April 10, 2019; revised May 17, 2019; accepted June 3, 2019

Abstract—A quantum chemical study of fluorinated europium alcoholate $Eu^{II}_2Eu^{III}(\mu\text{-}OR^F)_2(\mu_2\text{-}OR^F)_3(\mu_3\text{-}OR^F)_2(DME)_2$ (**I**), where DME is 1,2-dimethoxyethane, is performed. The structure of the complex contains numerous F···F, F···O, F···H, and C–F → Eu interactions. The nature and energy of these nonvalent interactions is studied in the framework of R. Bader's quantum theory "Atoms in Molecules." Nonvalent interactions between the negatively charged fluorine atoms in the structure of complex **I** can occur due to the donation of the electron density from the regions where the electron density is fairly highly concentrated to the regions of its relative depletion. Weaker C–F → Eu interactions are observed by the additional study using the Topos Pro structural topological program package. These interactions are confirmed by the study of the delocalization indices of electrons in the region of potential Eu···F interactions.

Keywords: F···F interactions, C–F → Eu interactions, halogen bond, quantum theory "Atoms in Molecules," ToposPro, delocalization indices

DOI: 10.1134/S1070328419110058

INTRODUCTION

Halogen bonds in which the "heavy" halogen atoms (I, Br, and Cl) participate as electron density acceptors are actively studied in the recent years [1–3]. These interactions are applied in molecular design. They can be used for the preparation of supramolecular chains or branched networks [4–8]. However, the $F^{\delta-}\cdots F^{\delta-}$ interactions are still interesting for research. There are numerous evidences for an increase in the volatility of the compounds upon the replacement of hydrogen atoms by fluorine atoms in the structure [9–12]. In several cases, fluorination leads to an increase in the enthalpy of sublimation and, correspondingly, to a decrease in the volatility of the compound compared to the non-fluorinated analog. For example, in the case of $C_{10}H_2F_{12}O_4Pb$, the enthalpy of sublimation is 111.7 ± 1.3 kJ/mol, whereas the enthalpy of sublimation is 102.4 ± 5.0 kJ/mol for the non-fluorinated analog $C_{10}H_{14}O_4Pb$ [13]. It is also known that the introduction of the F substituent can affect the biological activity of amino acids [14].

There are several works devoted directly to the study of the nature and energy of the F···F interactions [15–17]. It is shown for any halogen···halogen (Hal···Hal) interactions that the possibility of the interaction to occur depends substantially on the mutual arrangement of the atoms. These interactions can take place in the case of two geometric possibilities [18]. The first possibility appears when $\theta_1 \approx \theta_2$ (type I), where θ_1 and θ_2 are the C–$Hal^1\cdots Hal^2$ and $Hal^1\cdots Hal^2$–C angles, respectively. The second possibility for the Hal···Hal interaction to occur is observed at $\theta_1 \approx 180°$ and $\theta_2 \approx 90°$ (type II). The classification of halogen···halogen interactions is presented in Scheme 1.

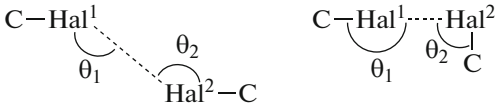

Type **I** Type **II**

Scheme 1.

It should be mentioned that the predominant number of these works is devoted to intermolecular interactions in organic or organoelement compounds with relatively "light" atoms (P, Cl). At the same time, it seems most interesting to study such interactions in the organometallic compounds, because the replacement of hydrogen atoms substantially affects the physicochemical properties of the complexes. In particular, a substantial change in the physicochemical properties of the coordination complexes of lanthanides can be expected upon fluorination. The Ln(III)/Ln(II) complexes due to possible *f*–*f*- and *f*–*d*-electron transitions can be used as emission materials [19, 20]. Many H–C fragments in the structure induce luminescence quenching, and the fluorination of the ligands is used as one of the methods preventing this phenomenon

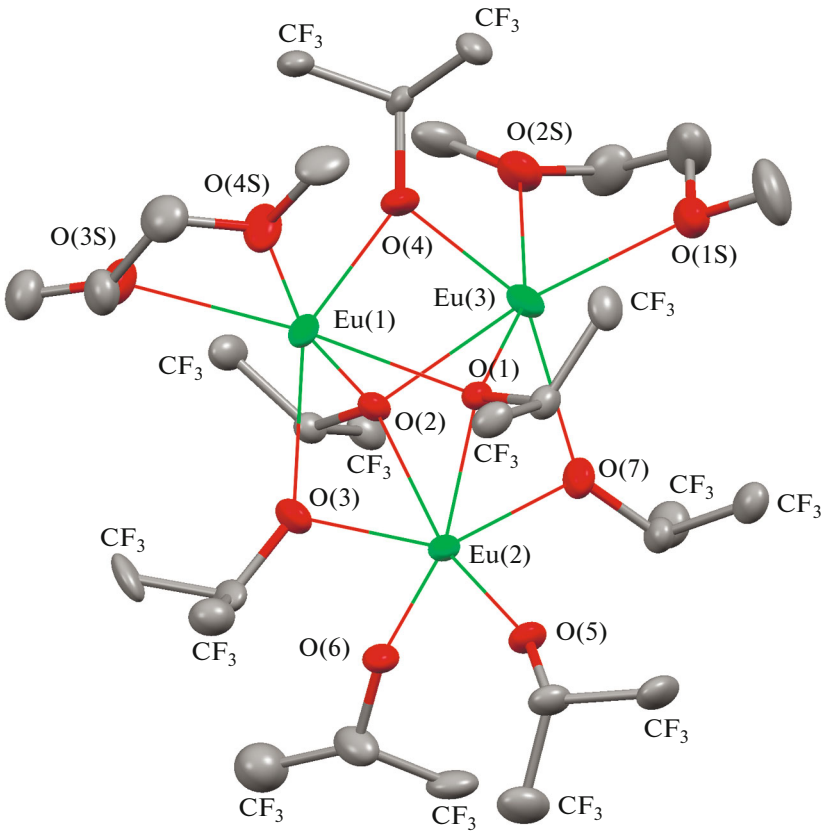

Fig. 1. Molecular structure of complex **I**. Thermal ellipsoids are shown with 30% probability. Hydrogen atoms are omitted for clarity.

[21]. In addition, intramolecular interactions C–F → Ln can occur in the structures with fluorinated ligands. The areas of application of these complexes are considerably extended due to such interactions. Presumably, some catalytic processes [22, 23] and decomposition of organolanthanide complexes [24, 25] start from the C–F → Ln interactions.

Thus, the study of noncovalent interactions in the structures of the organometallic complexes is an important task in the course of understanding a relation between the structure and physicochemical properties.

EXPERIMENTAL

The full geometry optimization of the $Eu^{II}_2Eu^{III}(\mu\text{-}OR^F)_2(\mu_2\text{-}OR^F)_3(\mu_3\text{-}OR^F)_2(DME)_2$ complex (**I**) was performed by the density functional theory (DFT) using the B3LYP hybrid functional in the Gaussian 09 program package [26]. The 6-31+G* basis set was used for the organic moiety, and the ECP28MWB pseudopotential was used for the europium atoms. The valence basis sets ((12s11p9d8f)/[9s8p6d5f]) with diffuse and polarization orbitals were used to describe the external shells of europium involved in chemical bond formation [27]. The electron density function for ECP was calculated using the Molden2aim program.

The topological analysis of the theoretical function of the electron density distribution was performed using the AIMALL program [28].

The calculations of delocalization indices (DI) and analysis of the deformation electron density (DED) for noncovalent interactions in complex **I** were performed using the Multiwfn v. 3.3.8 program [29]. The 3*d* distribution of the DED was visualized using the GPView program [30].

The geometric analysis of intramolecular Eu···F interactions was carried out using the ToposPro 5.0.2.1 structural topological program package [31] and the AutoCN module (method of spherical sectors [32], MinOm = 0.50).

RESULTS AND DISCUSSION

Europium complex **I** was chosen as the main object of the study. The synthesis procedure and the detailed study of the crystal structure of complex **I** were described [33]. The molecular structure of the complex is presented in Fig. 1.

Many closely arranged fluorine atoms in the molecule of complex **I** suggest intramolecular F···F interactions in the structure. To check this hypothesis, we performed the quantum chemical study of complex **I**.

Table 1. Comparison of the experimental and calculated Eu–X (X = O, F, Eu) bond lengths in complex **I**

Bond	Eu–$X_{X\text{-ray}}$, Å	Eu–X_{calc}, Å	Δ	Bond	Eu–$X_{X\text{-ray}}$, Å	Eu–X_{calc}, Å	Δ
Eu(1)–O(1)	2.520(4)	2.5313	0.011	Eu(2)–O(7)	2.333(3)	2.3401	0.007
Eu(1)–O(2)	2.740(4)	2.6667	0.073	Eu(3)–O(1)	2.738(4)	2.6820	0.056
Eu(1)–O(3)	2.532(3)	2.4760	0.056	Eu(3)–O(2)	2.513(4)	2.5390	0.026
Eu(1)–O(4)	2.469(4)	2.4683	0.001	Eu(3)–O(4)	2.472(3)	2.4799	0.008
Eu(1)–O(3S)	2.640(3)	2.6793	0.039	Eu(3)–O(7)	2.519(3)	2.4817	0.037
Eu(1)–O(4S)	2.640(5)	2.7213	0.081	Eu(3)–O(1S)	2.630(5)	2.7909	0.161
Eu(1)–F(1)	2.920(4)	2.8690	0.051	Eu(3)–O(2S)	2.659(5)	2.7631	0.104
Eu(1)–F(10)	2.699(4)	2.7873	0.088	Eu(3)–F(4)	2.675(4)	2.7730	0.098
Eu(2)–O(1)	2.446(4)	2.4681	0.022	Eu(3)–F(7)	2.893(4)	2.8158	0.077
Eu(2)–O(2)	2.437(4)	2.4690	0.032	Eu(1)–Eu(2)	3.7172(4)	3.6991	0.018
Eu(2)–O(3)	2.331(4)	2.3500	0.019	Eu(1)–Eu(3)	3.8202(5)	3.7927	0.028
Eu(2)–O(5)	2.167(4)	2.1649	0.002	Eu(2)–Eu(3)	3.7096(5)	3.7061	0.004
Eu(2)–O(6)	2.160(4)	2.1472	0.013	Δ_{av}			0.045

The optimization performed satisfactorily reproduces the main geometric characteristics of the complex and can be used for further calculations (Table 1). The average deviation of the Eu–X (X = O, F, Eu) bonds is 0.045 Å. The highest changes are observed for the Eu–O(DME) bonds. Evidently, this is related to the coordination character of the interaction and to the influence of the packing effect on this distance in crystal.

The Eu(1) and Eu(3) atoms in complex **I** are divalent, whereas Eu(2) has the formal charge +3. This representation is well consistent with the atomic charges calculated using the AIMALL program [28]. All fluorine and oxygen atoms in complex **I** have the negative charge, whereas all carbon and hydrogen atoms are positively charged (Table 2).

The study of the topology of the electron density (ED) in complex **I** using the AIMALL program [28] shows that all Eu(II)–O and Eu(II)···F interactions correspond to the type of closed shells ($\nabla^2\rho(\mathbf{r}) > 0$, $h_e(\mathbf{r}) > 0$. In turn, all bonds of Eu3+ with the terminal and μ-2-bridging O-*iso*-PrF ligands represent the type of intermediate interactions ($\nabla^2\rho(\mathbf{r}) > 0$, $h_e(\mathbf{r}) < 0$ (Table 3).

An interesting feature of the structure is the presence of numerous intramolecular nonvalent interactions. The dative C–F → Eu interactions should be assigned to important structural features (Fig. 2a). In the framework of R. Bader's quantum theory "Atoms in Molecules" (AIM) [34], we found four intramolecular F···Eu interactions in the structure of complex **I** (Table 4).

According to the Espinosa–Molins–Lecomte correlations [35], the energy of these interactions ranges from 3.92 to 5.07 kcal/mol, which is only insignificantly lower than the corresponding values for the Eu–O(DME) coordination bonds (5.44–7.28 kcal/mol). For comparison, the energy of Eu–O(*iso*-Pr^F) varies from 7.33 to 37.56 kcal/mol on going from the μ_3-bridging to terminal ligands. Thus, these four Eu–F interactions should undoubtedly be taken into account when determining the coordination number and coordination environment of the lanthanide atom.

However, along with four Eu–F interactions, which were localized by the study of the ED topology, five shortened Eu···F distances (3.305–3.691 Å) are observed in the structure of complex **I**. These geometric parameters indicate a possible interaction between the europium and fluorine atoms [36]. The geometrical topological analysis using the ToposPro structural topological program package [31] confirmed the presence of four strong Eu–F interactions found in the framework of the AIM approach. In addition, the ToposPro computational analysis revealed five weaker Eu···F interactions (Table 4).

Interestingly, the contacts with solid angles (SA) of 8.39–11.35% correspond to the interactions confirmed by the AIM method. At the same time, the remained five Eu···F interactions correspond to much

Table 2. Atomic charges in complex **I**

Atom	Charge, e
Eu(1)	1.68
Eu(2)	2.16
Eu(3)	1.67
q(F)	–0.65...–0.63
q(C)	0.43–1.74
q(O)	–1.24...–1.09
q(H)	0.02–0.12

Table 3. Selected topological characteristics of the Eu–O and Eu···F bonds in complex **I**

Bond	$v(\mathbf{r})$, au	$\rho(\mathbf{r})$, au	$\nabla^2\rho(\mathbf{r})$, au	$h_e(\mathbf{r})$, au	E_{EML} [35], kcal/mol
Eu(1)–O(1)	–0.036	0.037	0.155	0.001	11.28
Eu(1)–O(2)	–0.024	0.028	0.108	0.001	7.67
Eu(1)–O(3)	–0.042	0.041	0.179	0.002	13.07
Eu(1)–O(4)	–0.042	0.041	0.183	0.002	13.15
Eu(1)–O(3S)	–0.023	0.026	0.106	0.002	7.28
Eu(1)–O(4S)	–0.021	0.024	0.095	0.002	6.44
Eu(1)–F(1)	–0.012	0.013	0.064	0.002	3.92
Eu(1)–F(10)	–0.015	0.016	0.076	0.002	4.85
Eu(2)–O(1)	–0.044	0.045	0.179	0.0004	13.74
Eu(2)–O(2)	–0.044	0.045	0.178	0.0003	13.73
Eu(2)–O(3)	–0.062	0.057	0.241	–0.001	19.50
Eu(2)–O(5)	–0.113	0.082	0.396	–0.007	35.47
Eu(2)–O(6)	–0.120	0.084	0.417	–0.008	37.56
Eu(2)–O(7)	–0.063	0.058	0.249	–0.001	19.91
Eu(3)–O(1)	–0.023	0.027	0.103	0.001	7.33
Eu(3)–O(2)	–0.035	0.037	0.151	0.001	10.94
Eu(3)–O(4)	–0.042	0.042	0.177	0.001	13.25
Eu(3)–O(7)	–0.042	0.042	0.176	0.001	13.14
Eu(3)–O(1S)	–0.017	0.021	0.080	0.001	5.44
Eu(3)–O(2S)	–0.019	0.022	0.087	0.002	5.81
Eu(3)–F(4)	–0.016	0.017	0.079	0.002	5.07
Eu(3)–F(7)	–0.015	0.015	0.072	0.002	4.59

Table 4. Intramolecular Eu···F interactions in complex **I**

Contact	$Eu\cdots F_{X\text{-}ray}$, Å	$Eu\cdots F_{calc}$, Å	E_{EML} [35], kcal/mol	SA*, %	DI, e
Eu(3)–F(4)	2.675(4)	2.7730	5.07	11.35	0.296
Eu(1)–F(10)	2.699(4)	2.7873	4.84	11.11	0.294
Eu(3)–F(7)	2.893(4)	2.8158	4.59	8.28	0.284
Eu(1)–F(1)	2.920(4)	2.8690	3.92	8.39	0.269
Eu(1)···F(21)	3.305	3.4228		3.36	0.111
Eu(3)···F(24)	3.343	3.4182		3.21	0.111
Eu(3)···F(42)	3.447	3.2248		2.89	0.166
Eu(1)···F(13)	3.543	3.4635		0.91	0.018
Eu(2)···F(9)	3.691	3.6528		0.52	0.061

* SA is the solid angle corresponding to the interaction calculated using the ToposPro program [31].

lower values of solid angles (0.52–3.36%). We calculated the DI to elucidate the real number of electrons delocalized between the europium and fluorine atoms in complex **I** and to confirm the possibility of interactions between these atoms [29]. It was found that DI = 0.27–0.30 e in the region of Eu···F interactions, which was confirmed both geometrically and by the ED analysis. The values of DI were much lower (0.06–0.17 e) in the region of C–F → Eu interactions that were found using ToposPro and were not localized in the framework of the AIM approach. However, it should be mentioned that this number of delocalized electrons is substantial (Table 4) compared to the pairs of noninteracting atoms (DI < 10^{-5} e) and confirms an

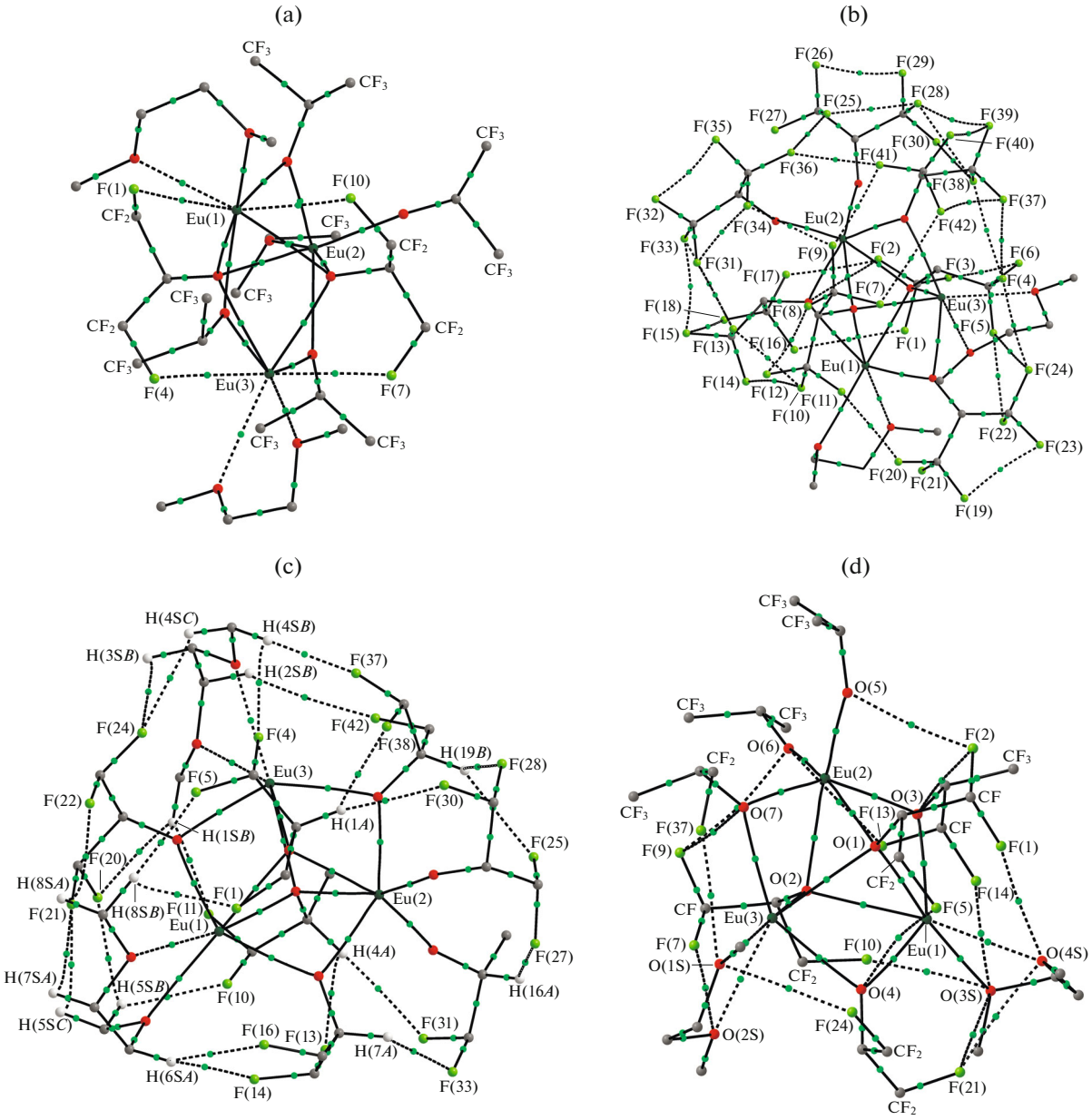

Fig. 2. Molecular graph of complex **I** (only CP(3, –1) for the (a) F···Eu, (b) F···F, (c) F···H, and (d) F···O interactions are presented particularly in the figures. The F and H atoms that are not involved in the corresponding interactions are omitted for clarity).

interaction between the europium and fluorine atoms in all nine cases.

An analysis of the DED shows that both strong (Fig. 3a) and weak (Fig 3b) Eu···F interactions in complex **I** are due to the donation of the ED from the region of its concentration on the fluorine atom to the positively charged europium atom. Thus, the complex study of the SA, DI, and DED confirms the existence of nine C–F → Eu interactions in complex **I**. It should be mentioned that the values of SA and DI for the found interactions indicate that the energy of interaction should be substantially higher for the Eu(1)–F(1), Eu(1)–F(10), Eu(3)–F(4), and Eu(3)–F(7) contacts.

Numerous intramolecular nonvalent interactions F···F, F···H, and F···O (Figs. 2b–2d) were observed in the structure of complex **I** together with the dative C–F → Eu interactions. The study of the ED topology made it possible to reveal the following interactions: 31 F···F, 24 F···H, and 14 F···O. Interestingly, each fluorine atom in the structure of complex **I** participates in at least one nonvalent interaction. The maximum number of such additional interactions is five for the structure of compound **I**. The same fluorine atom acts

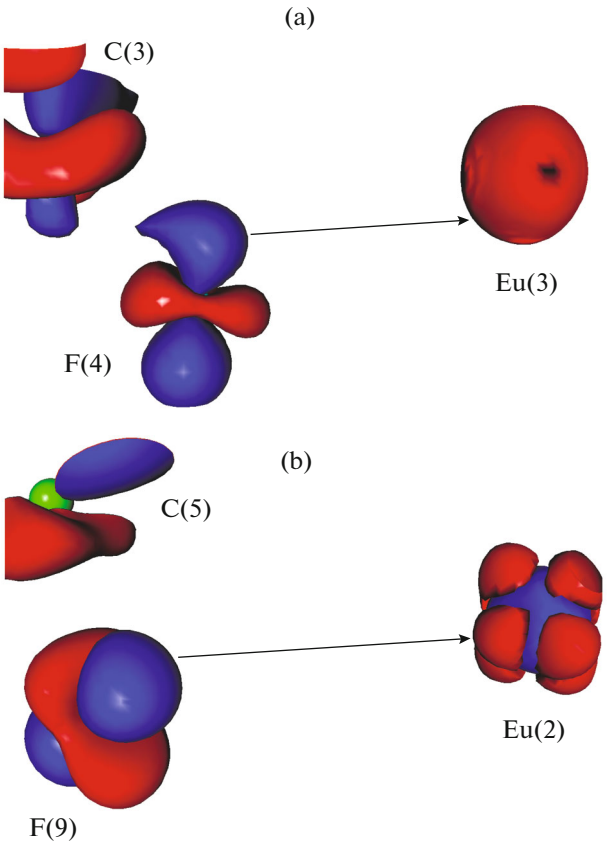

Fig. 3. 3*d* Distribution of the DED (0.05 au) in complex **I** in the regions corresponding to the (a) C(3)–F(4) → Eu(3) and (b) C(5)–F(9) → Eu(2) interactions. Blue color corresponds to the region of ED concentration, and the region of ED depletion is red-colored.

as both the ED donor (Figs. 4a, 4b) and ED acceptor (Figs. 4c–4e)

An analysis of the geometry of halogen interactions showed that the majority of the F···F interactions in complex **I** can be attributed to type I (Scheme 1). It should be mentioned that all F···H interactions in the structure of complex **I** can conventionally be assigned to either type I ($\theta_1 \approx \theta_2$), or type II ($\theta_1 \approx 90°$, $\theta_2 \approx 180°$) according to the geometrical criteria. The major part of the F···H interactions in the structure of complex **I** is also of type I.

The distances for the F···F, F···H, and F···O interactions in complex **I** vary in fairly wide ranges (2.654–3.196, 2.235–3.197, and 2.777–3.448 Å, respectively). Thus, the scatter in energies of the corresponding interactions is also significant (0.67–4.10, 0.19–3.25, and 0.51–3.03 kcal/mol) (Table 5). The total contribution of all $F^{\delta-}\cdots F^{\delta-}$ interactions to the stabilization of the molecular structure of complex **I** is 81.86 kcal/mol. This value exceeds the total contribution of the $F^{\delta-}\cdots H^{\delta+}$ (43.26 kcal/mol) and $F^{\delta-}\cdots O^{\delta-}$ (25.19 kcal/mol) interactions.

The DI values were also calculated for all nonvalent F···X (X = O, F, H) interactions found by us in complex **I**. The values of DI were 0.001–0.019, 0.003–0.018, and 0.003–0.030 e for the F···O, F···H, and F···F interactions, respectively. These values substantially exceed the DI for the noninteracting atoms ($<10^{-5}$ e) and indicate an interaction between these atoms.

The distances between the atoms exceed the sum of the van der Waals radii of the elements for several F···X (X = O, F, H) interactions [37]. At the same time, the structure of complex **I** contains a series of F···F pairs for which the distance between the atoms lies inside the range of localized interactions. However, no critical point (CP) CP(3, –1) was observed. For example, the F(3)···F(5) distance is 3.0516 Å, and the bond route and CP(3, –1) are absent. The structure of complex **I** also exhibits several examples of F···F for which the distance between the atoms only insignificantly exceeds the range of localized interactions. For instance, this value is 3.3838 Å for the pair of atoms F(19)···F(22). It is interesting that for these interactions both the geometric ($\theta_1 = 69.50°$, $\theta_2 = 65.28°$ for F(3)···F(5), $\theta_1 = 60.09°$, $\theta_2 = 58.04°$ for F(19)···F(22)) and electronic factors (DI is 0.005 and 0.001 e for F(3)···F(5) and F(19)···F(22), respectively) indicate a possible interaction between the atoms. The study of the DED fragment also confirms this fact (Fig. 5). Thus, it can be concluded that the structure of complex **I** also contains weaker F···F interactions, which

Table 5. Selected geometric and topological characteristics corresponding to the intramolecular F···X (X = F, H, O) interactions in complex **I**

Interaction	Number	F···X_{calc}, Å	ρ(**r**), au	$\nabla^2\rho(\mathbf{r})$, au	E_{EML} [35], kcal/mol	DI, e	$\sum E$, kcal/mol
F···F	31	2.6535–3.1962	0.003–0.013	0.019–0.061	0.66–4.11	0.003–0.030	81.86
F···H	24	2.2350–3.1968	0.001–0.012	0.007–0.049	0.19–3.25	0.003–0.018	43.26
F···O	14	2.7769–3.4483	0.003–0.010	0.015–0.043	0.51–3.03	0.001–0.019	25.19

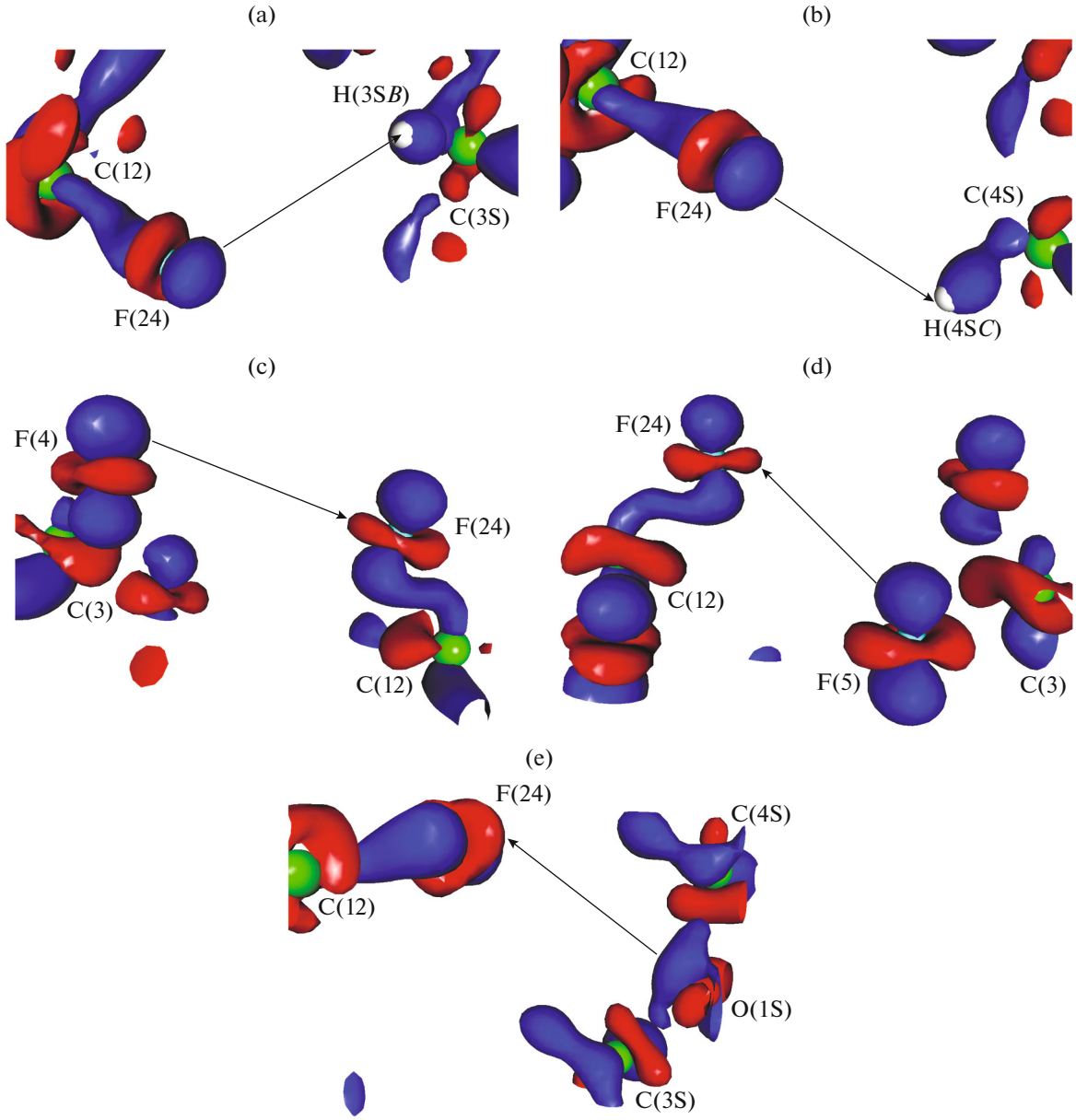

Fig. 4. 3*d* Distribution of the DED (0.05 au) in complex **I** in the regions corresponding to the (a) F(24)···H(3SB), (b) F(24)···H(4SC), (c) F(4)···F(24), (d) F(5)···F(24), and (e) F(24)···O(1S) interactions. Blue color corresponds to the region of ED concentration, and the region of ED depletion is red-colored.

cannot be localized in the framework of the AIM theory.

Three intramolecular O···H interactions of the intermediate type (3.66, 2.15, and 1.57 kcal/mol) are also observed in the structure of complex **I** along with the F···F, F···O, F···H, and C–F → Eu interactions.

Thus, the electronic structure of complex **I** and the nature and energy of the noncovalent interactions Eu···F, F···F, F···H, and F···O were studied. Four "strong" and five "weak" Eu···F interactions were found in the structure of complex **I**. The presence of all C–F → Eu interactions in compound **I** was confirmed by the calculations of the DI of electrons. The interactions of this type were shown to be caused by the ED donation from the region of its concentration on the fluorine atom to the positively charged lanthanide cation. The nature and energy of the following interactions in the structure of compound **I** were studied: 31 F···F, 24 F···H, and 14 F···O. The contribution of all $F^{\delta-}\cdots F^{\delta-}$ interactions in complex **I** to the stabilization of the molecular structure of the complex (81.86 kcal/mol) exceeds the total contribu-

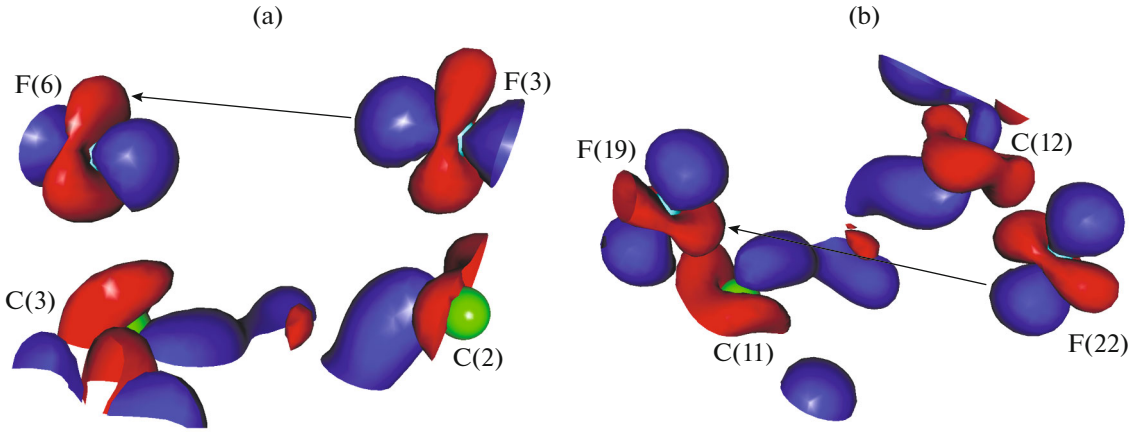

Fig. 5. 3*d* Distribution of the DED (0.05 au) in complex **I** in the regions corresponding to possible (a) F(3)···F(6) and (b) F(19)···F(22) interactions. Blue color corresponds to the region of ED concentration, and the region of ED depletion is red-colored.

tion of the $F^{\delta-}\cdots H^{\delta+}$ (43.26 kcal/mol) and $F^{\delta-}\cdots O^{\delta-}$ (25.19 kcal/mol) interactions. It is shown that the regions of ED concentration on one fluorine atom correspond to the regions of ED depletion on another atom for all localized F···F interactions.

FUNDING

This work was supported by the state task (theme no. 44.2, registration no. AAAA-A16-116122110053-1).

CONFLICT OF INTEREST

The authors declare that they have no conflict of interest.

REFERENCES

1. Bartashevich, E.V. and Tsirel'son, V.G., *Usp. Khim.*, 2014, vol. 83, no. 12, p. 1181.
2. Bartashevich, E.V., Yushina, I.D., Stash, A.I., and Tsirelson, V.G., *Cryst. Growth Des.*, 2014, vol. 14, no. 11, p. 5674.
3. Duarte, D.J.R., Peruchena, N.M., and Alkorta, I., *J. Phys. Chem. A*, 2015, vol. 119, no. 16, p. 3746.
4. Rissanen, K., *CrystEngComm*, 2008, vol. 10, p. 1107.
5. Gilday, L.C., Robinson, S.W., Barendt, T.A., et al., *Chem. Rev.*, 2015, vol. 115, p. 7118.
6. Priimagi, A., Cavallo, G., Metrangolo, P., and Resnati, G., *Acc. Chem. Res.*, 2013, vol. 46, no. 11, p. 2686.
7. Berger, G., Soubhye, J., and Meyer, F., *Polym. Chem.*, 2015, vol. 6, p. 3559.
8. Li, B., Zang, S.-Q., Wang, L.-Y., and Mak, Th.C.W., *Coord. Chem. Rev.*, 2016, vol. 308, p. 1.
9. Grushin, V.V., Herron, N., LeCloux, D.D., et al., *Chem. Commun.*, 2001, p. 1494.
10. Mancino, G., Ferguson, A.J., Beeby, A., et al., *J. Am. Chem. Soc.*, 2005, vol. 127, p. 524.
11. Tiitta, M. and Niinistou, L., *Chem. Vap. Deposition*, 1997, vol. 3, no. 4, p. 167.
12. Eisentraut, K.J. and Sievers, R.E., *J. Inorg. Nucl. Chem.*, 1967, vol. 29, p. 1931.
13. Krisyuk, V.V., Sysoev, S.V., Fedotova, N.E., et al., *Thermochim. Acta*, 1997, vol. 307, p. 107.
14. Smart, B.E., *J. Fluorine Chem.*, 2001, vol. 109, p. 3.
15. Osuna, R.M., Hernandez, V., Navarrete, J.T.L., et al., *Theor. Chem. Acc.*, 2011, vol. 128, p. 541.
16. Hathwar, V.R. and Row, T.N.G., *Cryst. Growth Des.*, 2011, vol. 11, p. 1338.
17. Karnoukhova, V.A., Fedyanin, I.V., and Lyssenko, K.A., *Struct. Chem.*, 2016, vol. 27, p. 17.
18. Ramasubbu, N., Parthasarathy, R., and Murray-Rust, P., *J. Am. Chem. Soc.*, 1986, vol. 108, p. 4308.
19. Bunzli, J.-C.G. and Piguet, C., *Chem. Soc. Rev.*, 2005, vol. 34, p. 1048.
20. Shipley, C.P., Capecchi, S., Salata, O.V., et al., *Adv. Mater.*, 1999, vol. 11, p. 533.
21. Glover, P.B., Bassett, A.P., Nockemann, P., et al., *Chem.-Eur. J.*, 2007, vol. 13, p. 6308.
22. Evans, W.J., Forrestal, K.J., Ansari, M.A., and Ziller, J.W., *J. Am. Chem. Soc.*, 1998, vol. 120, p. 2180.
23. Liu, B., Roisnel, T., Maron, L., et al., *Chem.-Eur. J.*, 2013, vol. 19, p. 3986.
24. Maleev, A.A., Fagin, A.A., Ilichev, V.A., et al., *J. Organomet. Chem.*, 2013, vol. 747, p. 126.
25. Melman, J.H., Rohde, C., Emge, T.J., and d Brennan, J.G., *Inorg. Chem.*, 2002, vol. 41, p. 28.
26. Frisch, M.J., Trucks, G.W., Schlegel, H.B., et al., *Gaussian 09*, Wallingford, 2009.
27. Dolg, M., Stoll, H., and Preuss, H., *J. Chem. Phys.*, 1989, vol. 90, p. 1730.
28. Keith, T.A., *AIMAll. Version 17.11.14. TK Gristmill Software*, Overland Park, 2017.
29. Lu, T. and Chen, F., *J. Comput. Chem.*, 2012, vol. 33, p. 580.
30. Shi, T. and Wang, P., *J. Mol. Graphics Modell.*, 2016, vol. 70, p. 305.

31. Blatov, V.A., Shevchenko, A.P., and Proserpio, D.M., *Cryst. Growth Des.*, 2014, vol. 14, p. 3576.
32. Peresypkina, E.V. and Blatov, V.A., *Acta Crystallogr., Sect. B: Struct. Sci.*, 2000, vol. 56, p. 1035.
33. Kuzyaev, D.M., Rumyantsev, R.V., Fukin, G.K., and Bochkarev, M.N., *Izv. Akad. Nauk. Ser. Khim.*, 2014, no. 4, p. 848.
34. Bader, R.F.W., *Atoms in Molecules—A Quantum Theory*, Oxford: Oxford Univ., 1990.
35. Espinosa, E., Molins, E., and Lecomte, C., *Chem. Phys. Lett.*, 1998, vol. 285, p. 170.
36. Rumyantsev, R.V. and Fukin G.K., *Izv. Akad. Nauk. Ser. Khim.*, 2017, no. 9, p. 1557.
37. Batsanov, S.S., *Neorg. Mater.*, 2001, vol. 37, no. 9, p. 1031.

Translated by E. Yablonskaya